Available on CMS information server

CMS CR -2024/319

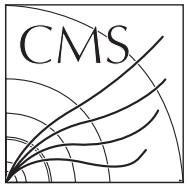

The Compact Muon Solenoid Experiment

Conference Report

Mailing address: CMS CERN, CH-1211 GENEVA 23, Switzerland

19 November 2024 (v3, 18 December 2024)

Forward Physics at LHC - Intersection with Astrophysics

Aldo Penzo for the CMS Collaboration

Abstract

LHC pp collisions at $\sqrt{s}$ = 14 TeV correspond to 100 PeV in the cosmic ray spectrum, reaching regions (such as the knee) whose interpretation is still debated, and whose models may be strongly influenced by LHC results on forward hadronic production, for instance as measured with CMS forward calorimeters. Other astrophysics problems that may receive a decisive input from LHC, and in particular HL-LHC, concern the interpretation of dark matter and dark energy in the universe, in correspondence with BSM particles that may be detected as LLP (Long-Lived-Particles). LLP searches have been generally done up to now at low pseudorapidity, as exemplified by some CMS recent results. There may be however reasons why detectors in the forward direction of LHC experiments, could be better suited for these searches, at least for some lifetime ranges, due to large relativistic boosts of the produced particles at LHC energies in the forward region. Considering the CMS forward detectors, their role for some of these searches and corresponding signatures are discussed. Additional possibilities of instrumenting specific regions of the LHC tunnel near the interaction point IP5, where CMS is installed, are discussed.

Presented at *QCD24 27th High Energy Physics International Conference in Quantum Chromodynamics*

Forward Physics at LHC: Intersections with Astrophysics

A. Penzo[1,2]
The University of Iowa, Iowa City, Iowa, USA

Abstract

LHC pp collisions at $\sqrt{s} = 14$TeV correspond to 10^{17}eV in the cosmic ray spectrum, reaching regions (f.i. the "knee") whose interpretation is still debated, and whose models may be strongly influenced by LHC results on forward hadronic production, for instance as measured with CMS forward calorimeters. Other astrophysics problems that may receive a decisive input from LHC, and in particular HL-LHC, concern the interpretation of dark matter and dark energy in the universe, in correspondence with BSM (Beyond Standard Model) particles that may be detected as LLP (Long-Lived Particles). LLP searches have been generally done up to now at low pseudorapidity η, as exemplified by some CMS recent results. There may be however reasons why detectors in the forward direction of LHC experiments, could be better suited for these searches, at least for some lifetime ranges, due to large relativistic boosts of the produced particles at LHC energies in the forward region. Considering the CMS forward detectors, their role for some of these searches and corresponding signatures are discussed. Additional possibilities of instrumenting specific regions of the LHC tunnel near the interaction point IP5, where CMS is installed, are discussed.

---

[1] Talk given at QCD24: 27th High Energy Physics International Conference in Quantum Chromodynamics, 8-12 Jul 2024, Montpellier (France)

[2] On behalf of the CMS Collaboration

1 Introduction

A few years ago, earlier in this conference series, a detailed report [1] has been given on the forward detectors of the Compact Muon Solenoid (CMS) experiment [2] at the Large Hadron Collider (LHC) [3] of CERN. Thanks to the huge center-of-mass energy $\sqrt{s} \approx 14$ TeV and luminosity $\geq 10^{34}\text{cm}^{-2}\text{s}^{-1}$ of LHC, its experiments have unprecedented physics reach [4–6], with good sensitivity even for extremely massive new particles, also if produced very rarely.

There are legitimate doubts, however, about the existence of such new particles, considering that the Higgs boson, discovered in 2012 [7, 8], provides the Standard Model (SM) [9–11] with its final capstone, but its measured mass ($m_H \approx 125$ GeV), much smaller than the Planck scale, $M_P \approx 10^{19}$ GeV, leads to tensions with the stability of the electroweak (EW) vacuum [12].

The "hierarchy" problem, together with GUT (Grand Unified Theory) schemes of forces' unification, could have as consequence the potential absence of new particles from the EW scale to near the Planck mass (the desert scenario), as sketched in Figure 1.

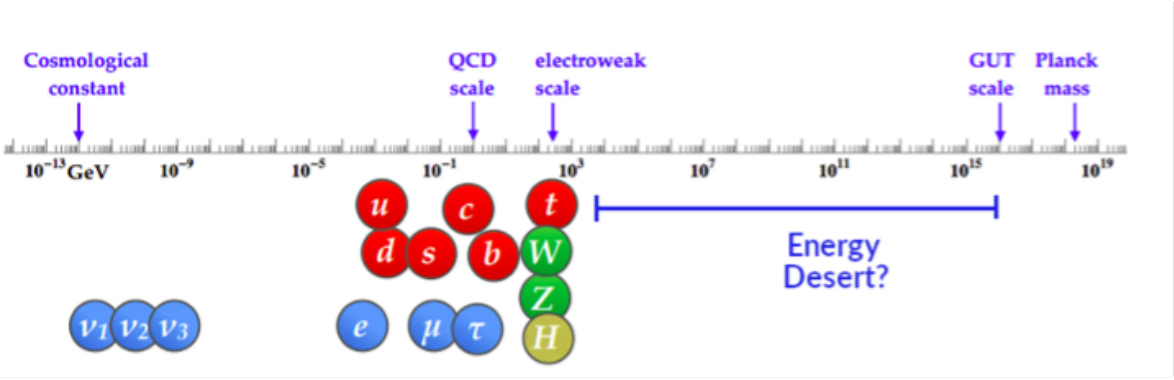

Figure 1: Particles' mass as a function of energy; maybe no new particles up to GUT or Planck scales?

This scenario might eventually be wrong, because the SM needs to be extended to explain gravity, dark matter, neutrino masses, inflation, and baryogenesis [13]. Another scenario, associated with the "hierarchy" problem, concerning the so-called "fine-tuning" of virtual contributions from massive particles to the Higgs mass, would imply the existence of particles beyond the Standard Model (BSM) with masses in an energy range accessible at the LHC [14].

Twelve years after the Higgs discovery, however, the LHC experiments seem to follow the first scenario, piling up results confirming the validity of SM with higher and higher precision, wiping away a few intriguing counter-indications [15], without reliable traces of BSM particles and new physics [16].

At this stage, it has been argued that new particles might escape observation, populating phase-space corners less equipped in the standard LHC experiments (for instance, the far-forward collision direction, along the beam pipes, or/and behaving in a drastically different manner than SM particles [17]). Particle constituents of Dark Matter (DM), whose existence is firmly implied by cosmic observations [18], in a proportion of 6:1 with respect to "ordinary" (SM) matter, are candidates for BSM particles coupling with SM particles very weakly, and therefore with a long lifetime prior to decaying to SM particles via special "portal" processes [19]. These long-lived particles (LLP) are actively being investigated, looking for new signatures [20].

2 Signal from Cosmos

On March 1610 in Venice, Galileo Galilei published a short treatise in Latin: *"Sidereus Nuncius"* [21] (Sidereal Messenger), containing his astronomical observations made with a telescope, an upgraded version of primitive image-enlarging devices (just a few times magnification) obtained by combining convex and concave lenses, developed in the Netherlands circa 1608. Having been informed about these devices, Galileo, in 1609, studied their principles and built improved versions, with more than ten-fold magnification, which he used for his early observations of mountains and craters on the Moon, hundreds of stars not visible to the naked eye in the Milky Way and other constellations, and the moons of Jupiter, which he named after the Medici family.

2.1 Birth of Modern Astronomy

The *"Sidereus Nuncius"* was the first publication of a novel experimental science of astronomy and the foundation for the present research with exceptionally powerful terrestrial [22] and space telescopes [23], having apertures many hundreds of times larger than Galileo's and magnifications reaching a few million times. Initially restricted to the visible spectrum, the technology rapidly evolved towards the use of the entire electromagnetic spectrum for astronomical observations [24].

2.2 Cosmic Rays: Origins and Observations

Other "sidereal messages" are reaching us through cosmic rays (CR), discovered in the 1910's by V. Hess with balloon-borne altitude measurements [25]. The first discoveries of subatomic particles beyond the proton, neutron, and electron, were obtained studying cosmic ray events: notably the positron, the first antiparticle (predicted by P. Dirac) discovered in 1932 [26] and then the muon [27] in 1936, initially confused with the Yukawa meson – both by C. Anderson and collaborators using cloud chambers. The pion, the real Yukawa meson, was discovered by C. Powell and collaborators [28], using emulsions. These results opened the field of modern particle physics and were followed by many other discoveries with cosmic rays. Only in the 1950's the baton for particle searches passed from cosmic rays to accelerators, with the antiproton production at the Bevatron of the Berkeley Radiation Laboratory [29].

2.3 Large Arrays for UHECR

Already in 1939, Pierre Auger and collaborators found evidence for extensive air showers (EAS), through coincidence between distant Geiger counters [30]. From the showers' lateral extension (larger than a football ground) and estimated number of particles, it could be deduced that the primary cosmic rays producing these cascades in the earth atmosphere could reach millions of GeV energies or higher; these ultra-high energy cosmic rays (UHECR) are quite rare (1 m^{-2} $year^{-1}$) and for their observation very large detectors' arrays have been deployed at ground level [31]: the largest and most recent arrays are the Pierre Auger Observatory and Telescope Array.

2.4 An Overall Picture: UHECR and Accelerators

In Figure 2, a comprehensive picture [32] summarizes the most significant features of the cosmic ray spectrum, consisting mainly of atomic nuclei (98%), 2% electrons and a small contribution of γ rays; out of the atomic nuclei, 87% are protons, 11% helium nuclei and 2% heavier nuclei. The energies of the primary cosmic rays range from around 1 GeV to as much as 10^8 TeV; the rate of these particles falls off with increasing energy, from about 1 m^{-2} s^{-1} at 100 GeV, to

about 1 m^{-2} y^{-1} at 3000 TeV (3 PeV), in the so-called "knee" region, and to 1 km^{-2} y^{-1} at 3×10^{18} eV (3 EeV) in the "ankle" region.

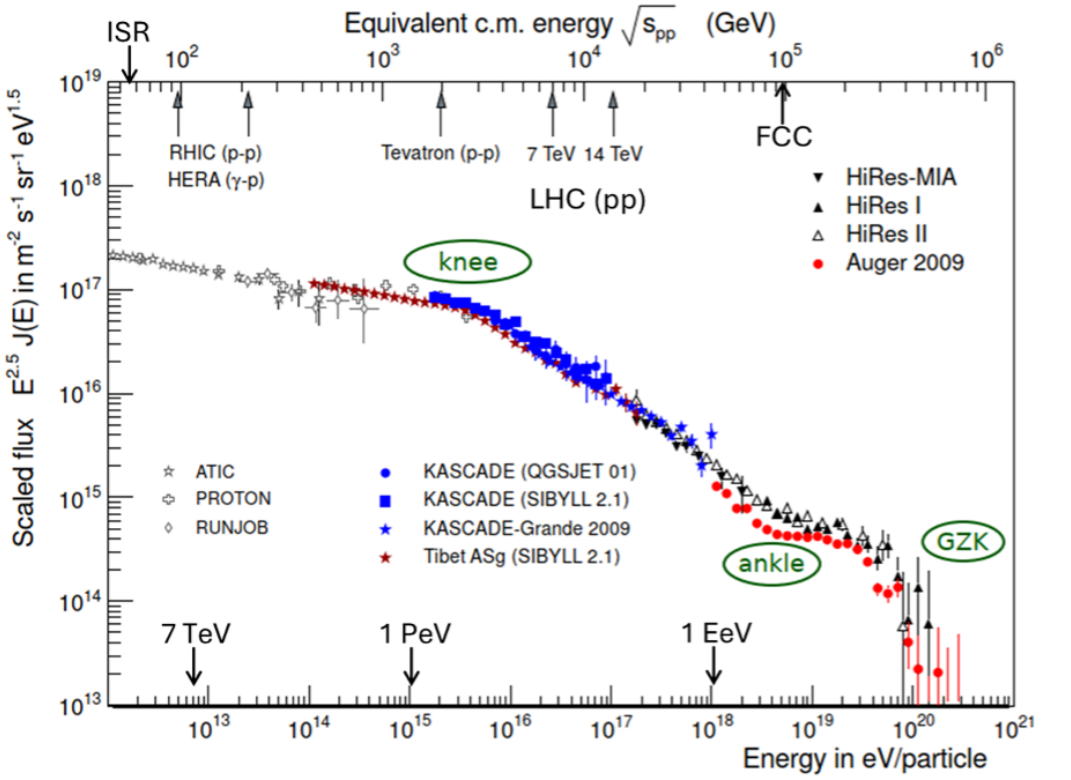

Figure 2: Cosmic rays' all-particle flux [32], scaled by $E^{2.5}$ to emphasize the most relevant features. The top axis indicates the equivalent center-of-mass (c.m.) energy for protons on Air, and for different pp colliders.

The energy spectrum can be described by a power law $E^{-\gamma}$, with a "spectral index" $\gamma \approx 2.7$ below the knee, and $\gamma \approx 3.1$ above. Another change in the spectral index is observed, in the so-called "ankle". For energies above $E \approx 10^{19}$ eV, a strong suppression of the flux is observed, attributed to the so-called "GZK-Cutoff" (Greisen-Zatsepin-Kuzmin) [33, 34] at an energy of $6 \cdot 10^{19}$ eV, due to interaction with photons of the cosmic microwave background (CMB). The knee may come from contributions of different nuclei (atomic number Z) in the primary flux, while, between the knee and the ankle, the onset of an extragalactic contribution could appear.

2.5 Space Detectors for Primary Cosmic Rays

In addition to the terrestrial arrays, the primary flux can be intercepted with satellite-borne detectors [35], notably Pamela, AMS, and CALET. Future progress in both fields of surface and space detectors is very significant: Auger and TA are expanding their coverage and instrumentation; in addition, a new concept of space observatory (POEMMA) is being designed, consisting of two identical satellites in loose formation at 525 km orbit altitude [36].

2.6 Cosmic Accelerators and Multi-Messenger Astrophysics

Astrophysicists and accelerator physicists are speculating over (and dreaming of…) mechanisms responsible for accelerating CR to such high energies: an intuition of E. Fermi [37] for achieving acceleration from random magnetic fields in the galaxies, has been developed with success, as described in a state-of-the-art recent review [38]. UHECR are a new type of

"Siderei Nuncii", together with high energy neutrinos, gamma-ray bursts and gravitational waves, studied with specialized detectors. The potential of combined analysis of multiple and complementary information sources (electromagnetic waves/photons from radio waves to gamma-rays, neutrinos, gravitational waves, and high-energy cosmic rays) has been fully appreciated and leveraged upon to provide new insights and to better understand the properties and processes of the most energetic events in the Universe, establishing a new discipline: Multi-Messenger Astrophysics [39].

3 Cosmic Rays and the LHC

The pp collider mode of LHC, providing a center-of-mass energy $\sqrt{s} \approx 14$ TeV, approaches the LHC range of energies to the "knee" region of the UHECR spectrum, which has a crucial role in the regime of cosmic rays. In fact, CR, mostly Hydrogen (protons) and Helium (α–particles) but occasionally even Fe-nuclei ($A \approx 1, 4, 56$), impact on air, a mixture composed (at sea level) mainly by Nitrogen ($\approx$ 78%) and Oxygen ($\approx$ 20%) plus traces of Argon and other gases, are like "fixed target" (FT) A_1-A_2 ions' collisions, with $A_{\rm Air} \approx 14.5$ (average over air composition) and $A_1 \approx 1, 4, 56$ (according to the incident nucleus).

3.1 Calorimetry at top of the Atmosphere and Underground

Considering the atmosphere as a large calorimeter for CR, the fundamental parameters are the air radiation length X_0 and absorption length $\lambda_{\rm abs}$ ($X_0 \approx 36.6\,{\rm g/cm^2}$, $\lambda_{\rm abs} \approx 61.3\,{\rm g/cm^2}$ values at sea level, pressure 1 atm, to be scaled with altitude), which determine the development of the EM and HAD (hadron) showers, and in particular the depth of the shower max, $X_{\rm max}$. The attenuation length $\lambda_a(E)$ is connected with the interaction length $\lambda_{p-{\rm air}}(E)$ by the relation:

$$\lambda_a(E) = k(E)\lambda_{p-{\rm air}}(E) = k(E)\frac{\langle A_{\rm air}\rangle m_p}{\sigma^i_{p-{\rm air}}(E)} \tag{1}$$

$k(E)$ is a model-dependent proportional factor, which among others depends on the mean inelasticity of the interactions; $\sigma^i_{p-{\rm air}}(E)$ is the total inelastic proton-air cross-section, $\langle A_{\rm air}\rangle = 14.5$, the effective atomic weight of air, and m_p the proton mass [40].

The parameters that control the physical processes involved in the shower development are equivalent for fixed target and collider at the same value of $\sqrt{s}$; in this sense, the LHC and cosmic rays at the "knee" are comparable. Collisions of heavy ions (Pb-Pb) at LHC reach full c.m. energy $\sqrt{s}$ larger than 1000 TeV, breaking the symbolic PeV barrier. For individual NN interactions (using the Glauber model [41]) $\sqrt{s_{NN}} \approx 2.76$ TeV. At these c.m. energies at LHC, the pp reactions tend to produce a large amount of particles, concentrated at relatively small pseudorapidity η, but the particles moving to larger η tend to carry much more energy (see Figure 3, left); in Pb-Pb interactions, the (global) energies involved are much higher, and the energy spectrum of the forward calorimeters HF reaches 130 TeV (see Figure 3, right).

3.2 CMS Forward Physics and Astrophysics issues

The general impact of LHC physics on cosmic rays' studies is considered here from the perspective of the Compact Muon Solenoid (CMS), described in [2]. The central part of CMS covers a pseudorapidity range $|\eta| < 3$. In the forward region, CMS was complemented by several subdetectors designed for events with activity at small angles, as described in [1]. A part of this

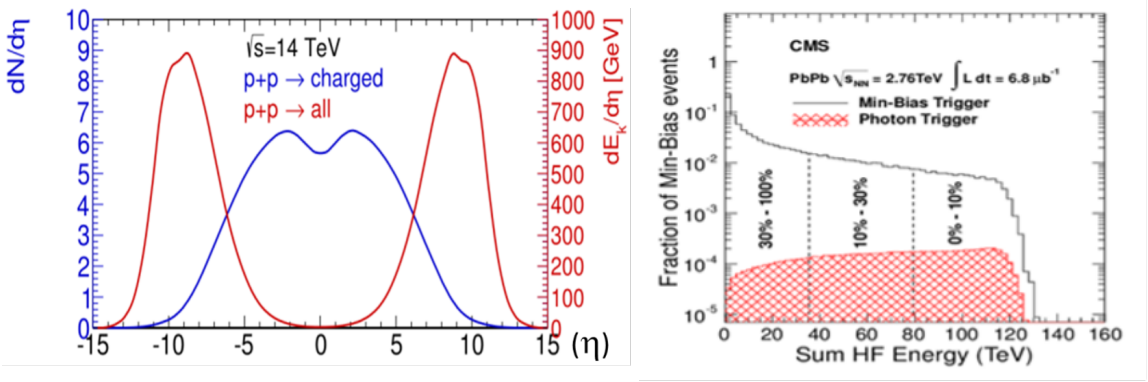

Figure 3: (Left) Distribution of (charged) particles' and energy flow in pp collisions at 14 TeV; most of the charged particles tend to concentrate in a central η-region, while energy flows to a large-η region. (Right) Total HF energy for minimum-bias PbPb collisions; the three regions separated by vertical dotted lines correspond to "centrality" ranges. The HF energy spectrum extends to about 130 TeV [42].

equipment has been discontinued or decommissioned due to radiation damage or rate saturation in the ever-increasing luminosity regime of runs 2 and 3. The forward hadron calorimeter (HF) has survived the multiplied luminosity thanks to a radiation-hard design and construction. Another apparatus that has taken the challenge to operate at full LHC regime in the very forward direction is the Roman Pots detector system, built and operated by the TOTEM team [43], and now merged in CMS as the Precision Proton Spectrometer (PPS), recently approved for the HL-LHC runs [44]. TOTEM has completed a campaign of measurements of total, elastic, and inelastic pp cross sections at different LHC energies [45].

3.3 LHC Forward Physics and Cosmic Rays

The TOTEM data reach an unprecedented precision (Table 2) in the fundamental cross-sections (Figure 4, right) that not only represent a challenge to the current high energy models of elastic scattering and diffraction, and give evidence for the elusive Odderon [46], but also provide leverage towards the cosmic-rays regime of energies, as shown by comparison with the data from the Pierre Auger observatory, particularly concerning the inelastic cross section (Figure 4, left), which contributes to the collision length, a fundamental parameter for the development of cosmic rays' showers in the atmosphere, as discussed above.

	$\mathcal{L}$ independent method			
	$\sqrt{2.76}$ TeV	$\sqrt{7}$ TeV	$\sqrt{8}$ TeV	$\sqrt{13}$ TeV
σ_{tot} (mb)	84.7 ± 3.3	98.0 ± 2.5	101.7 ± 2.9	110.6 ± 3.4
σ_{inel} (mb)	62.8 ± 2.9	72.9 ± 1.5	74.7 ± 1.7	79.5 ± 1.8
σ_{el} (mb)	21.8 ± 1.4	25.1 ± 1.1	27.1 ± 1.4	31.0 ± 1.7

Table 1: Latest results for pp cross section TOTEM measurements at LHC [45]

The pp inelastic cross section, via the Glauber model [41], can provide the p-Air cross section, which is extracted from the cosmic ray showers' parameters.

In line with the considerations about the nuclear composition of the CR projectiles, and of the target (Air), it is interesting to consider also the p-Pb interactions [47] in LHC (Figure 5); of course, the air composition would be better approached with lighter ions, for instance, Oxygen, which is foreseen in special runs during Run 3.

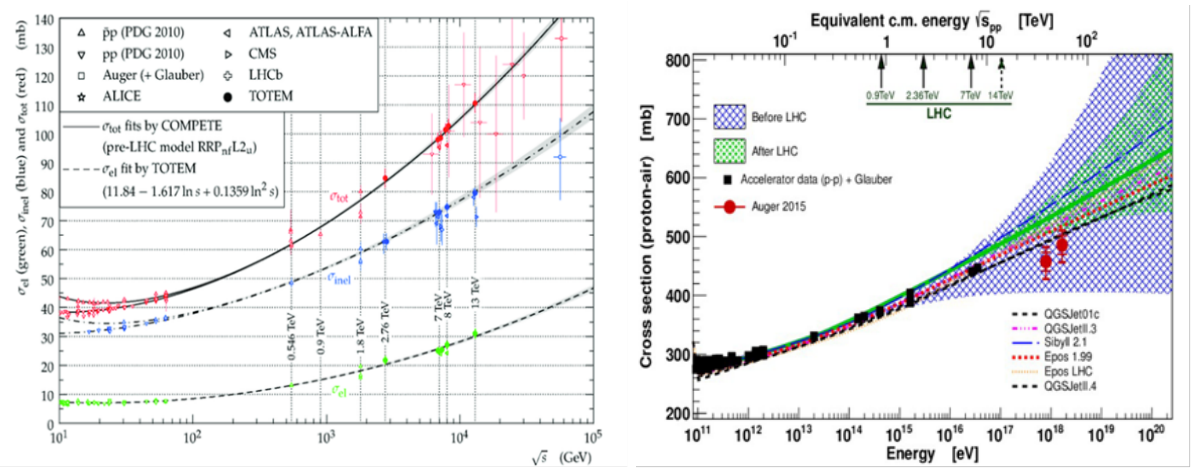

Figure 4: (Left) Latest results for proton-proton Cross Section Measurements with the TOTEM experiment at LHC. (Right) The energy dependence of σ_{inel} is displayed for data before LHC (including the Tevatron) and data from LHC. Data from Auger observatory (red) are shown.

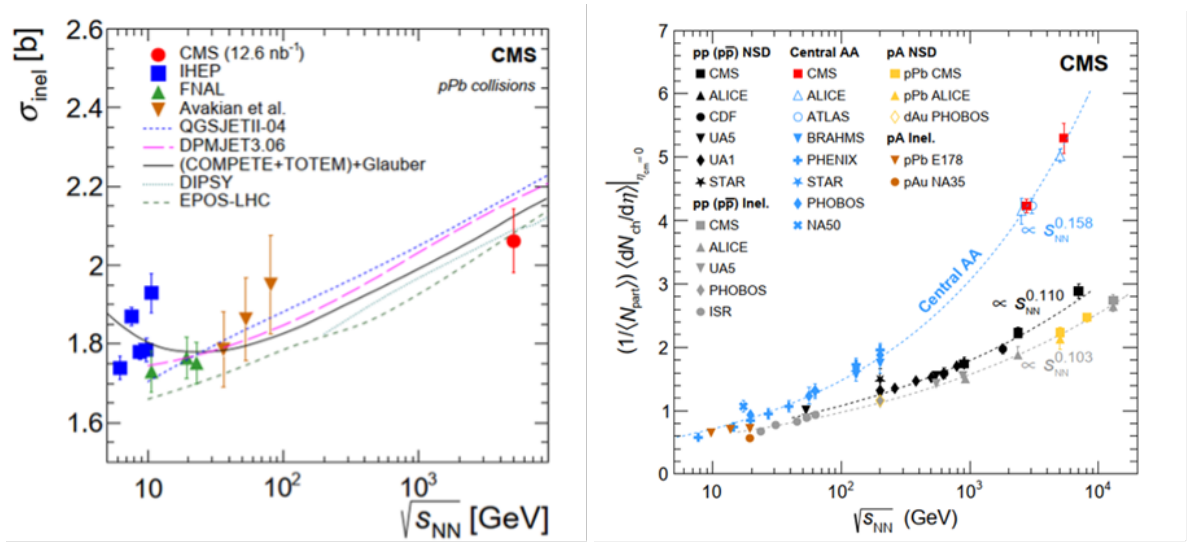

Figure 5: (Left) Inelastic cross sections for pPb collisions as a function of the c.m. energy. The CMS measurement (red circle) is compared to lower energy data and different model predictions. (Right) Comparison of average $dN_{ch}/d\eta$ at midrapidity for pA (Pb, Au) and dAu, as well as central HI collisions and non-single-diffractive (NSD) and inelastic pp collisions.

The value of $\sigma^{\text{inel}}(\text{pPb})$ is compatible with that expected from pp at 5.02 TeV, scaled up within a Glauber approach [41] to account for multiple scatterings in the Lead nucleus, indicating that further net nuclear corrections are small. An important synergy aspect between UHECR observatories and accelerator/collider experiments consists in a systematic approaching of experimental and analysis methods of the two communities in order to allow safe extrapolations in energy (from $\sqrt{s} \sim 14$ TeV up to $\sqrt{s} \sim 400$ TeV), forward phase space regions, and projectile and target particle combinations. Different features of forward detectors at LHC have been considered in this perspective for CMS [48, 49] and ATLAS [50]. A remarkable effort has been made to tune the MC generators for EAS with measurements at LHC [51, 52]. As shown in Figure 4 (right), the evaluations of $\sigma^{\text{inel}}_{\text{p-Air}}$ from LHC and Auger are compatible and the retuned simulation programs tend to converge also at ultra-high energies. In this respect, it could have been considered possible not only to use keys from LHC to interpret CR behaviour, but, recip-

rocally, to test hadronic interactions at ultrahigh energies with CR, providing an exceptionally wide stage for QCD phenomenology in extreme conditions [53]. The increased reliability of simulation programs, however, has emphasized conflicting points [54], leading to discrepancies or anomalies that remain as open questions [55] to be solved before assuming congruence of the two regimes.

3.4 The muon puzzle

This situation is clearly exemplified in Figure 6: the right plot shows $\langle X_{\max} \rangle$, the mean of EAS shower-max as a function of energy from various observatories, which are in good agreement, and contained between the expected lines for protons and Fe, with a possible trend towards higher Z with energy. The right plot gives the average muon content $\langle R_\mu \rangle$ per shower energy $E/10^{19}$ eV as a function of shower energy E. The brackets indicate systematic uncertainties and shifts due to 14% energy scale uncertainty. Theoretical curves for proton and iron showers are shown for comparison. This muon puzzle is a serious problem as it is very difficult to increase the number of muons by such a large fraction just changing the physics of the first interaction.

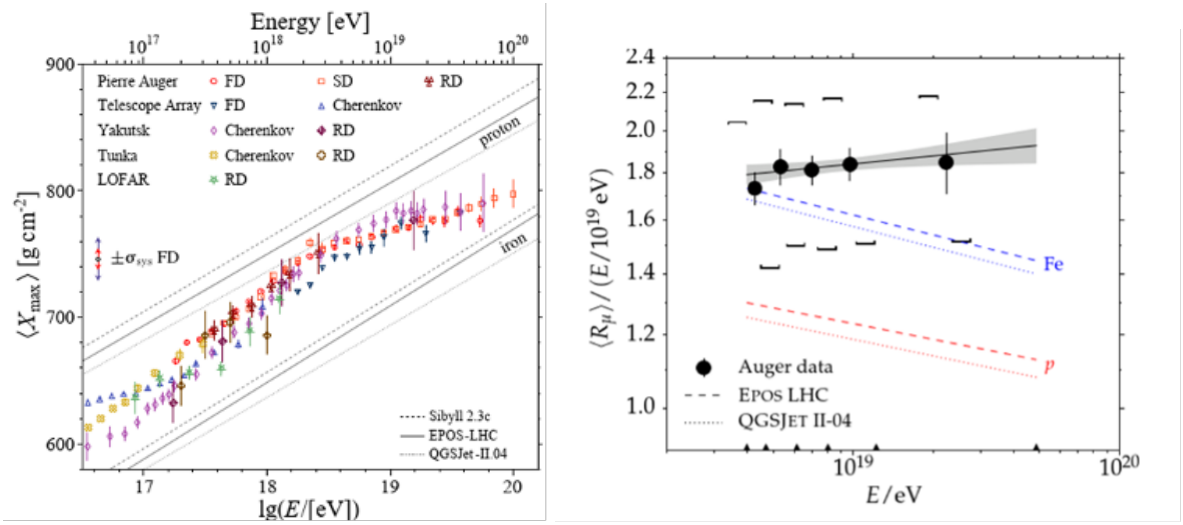

Figure 6: (Left) The mean of the shower maximum $\langle X_{\max} \rangle$, as a function of energy from various observatories. The results are in good agreement, and well contained between the expected lines for protons and Fe, with a possible trend towards higher Z with energy. (Right) Average muon content $\langle R_\mu \rangle$ per shower energy $E/10^{19}$ eV as a function of the shower energy. The brackets indicate systematic uncertainties and shifts. Theoretical curves for proton and Fe showers are shown for comparison.

The muon excess [56] has been interpreted in many ways [57]; contributions from hard QCD jets and heavy-quarks production do not seem to account fully for the excess [54]; another solution to decrease the EM shower component, coming from π^0 decays, would be through a partial replacement of pions (notably π^0's) by K (strange mesons), attributed [58, 59] to "strangeness enhancement," which is considered a signature of QGP (Quark-Gluon Plasma) formation in nuclear collisions and has been observed initially in fixed target nuclear interactions [60] and more recently in PbPb and pp collisions [61] at LHC. It is not clear if this hypothesis can explain the muon puzzle; however, the muon excess appears at a TeV scale, suggesting that this deviation may be observable at the LHC, in particular with ions lighter than Pb: there are plans to use Oxygen in LHC towards the end of Run 3. CMS has data for pp and pPb collisions at $\sqrt{s_{\rm NN}} = 5.02$ TeV [62], showing an enhancement effect and a mass ordering in the same way as [61].

4 Another Sidereal Message: Dark Matter

The need of additional (invisible) mass to hold together galaxies and clusters of galaxies in rapid rotation was noticed already in the 1930's by F. Zwicky [63], who called it "dunkle Materie," in opposition to luminous matter. However, only in the 1970's, more extended observations [64] led to general consensus on the existence of large quantities, outweighing visible matter roughly six to one, of gravitational matter not interacting electromagnetically.

4.1 Dark Matter at LHC

Dark matter particles, if produced at LHC, even if not interacting with the apparatus, might have signatures of missing energy and transverse momentum; dark matter candidates may be associated with BSM theories and models, such as Supersymmetry [65], for instance; many of these models include long-lived particles (LLP), which could manifest themselves with striking unconventional signatures [20]. A review of DM searches at LHC is given in [66]; recently a complete report on DM studies in CMS [67] has been submitted to Physics Reports.

Here certain specific signatures are discussed in the context of the forward apparatus in CMS, as it has been evolving during the Run 3 and in the perspective of the HL-LHC era.

With respect to the situation of the forward CMS region at the earlier stages of LHC, as described in [1], part of the equipment has suffered radiation damage or rate saturation in the ever-increasing luminosity regime in runs 2 and 3, and has been discontinued or decommissioned: of the detectors described in [1], only the forward hadron calorimeter HF has survived the boost in luminosity.

4.2 The Hadron Forward (HF) Calorimeters

The forward calorimeters (HF), located 11 m from IP5, at large pseudorapidity ($3 \leq |\eta| \leq 5.2$) in CMS, are essential for physics channels with missing transverse energy E_T, significantly improving the hermeticity of the experiment [1]. HF also play a prominent role in detecting forward "tagging" jets in vector boson fusion/scattering (VBF/VBS) processes [68]. VBF is a specific mechanism for Higgs production, which has played a significant role in the discovery of the Higgs and is expected to have even more importance in studies of "invisible" decays of the Higgs as a "portal" for the dark sector [19], or for searches of heavier Higgs' partners [69].

In view of the challenging radiation flow in the HF, fused-silica (SiO_2) optical fibers, known for their exceptional radiation hardness [70], were chosen as active (Cherenkov-emitting) elements, embedded in steel absorbers. Thus, the detectors are preferentially sensitive to the electromagnetic core of the showers and, as hadronic calorimeters, are highly non-compensating (e/h $\approx$ 5). This feature is also manifest in measured shower profiles that are rather narrow and relatively short with a typical scale X_0 (Rad. Length), even at TeV energies, compared to similar calorimeters based on ionization [1], with a scale λ_I (Int. length), almost 10 times larger. Fibers are read out with metal-channel multianode photomultipliers (R7600U-100-M4 PMT) from Hamamatsu. Due to the sharp Cherenkov emission from the fibers and the excellent time definition of the PMTs, the combination of SiO_2 fibers and R7600 PMTs provides high precision timing, typically $\leq$ 250 ps, over the almost 9 m^3 volume of the calorimeters.

These known features of HF have been recently investigated using high-resolution readout developed for ToF measurements at 10-25 ps levels with quartz bars [71]. With this system, it has been possible to demonstrate that arrays made with HF fibers, in high-energy (typically 180 GeV/c) electron or hadron beams, can reach 25 ps ToF resolution with MCP-PMTs and 150 ps with PMTs of the same family as those installed in HF.

4.3 LLP calorimeter signatures

Among a large number of LLP signatures at LHC [72], it has been noted that detectors with excellent time resolution, planned to be inserted within LHC experiments (timing layers) to mitigate the high pile-up problems at HL-LHC[73], distinguishing between interaction points in the same bunch-crossing through small time differences, could also provide a signature for LLP candidates, by spotting their decay products, delayed with respect to the swarm of prompt particles ($\beta \approx 1$) from the IP, by a potentially slower motion of the LLP up to the decay position, and the additional time for the decay products to reach the detectors [74]. This method has been applied to the CMS ECAL, relying on its time measuring capabilities [75], for searching delayed jets produced by displaced decays of heavy LLP within or nearby the ECAL [76]. This approach is considered to have significant sensitivity, with high efficiency for jet identification and missing p_T measurement; backgrounds from satellite bunch collisions, beam halo and cosmic muons, are estimated to be negligible. A benchmark model of gluino production and decay is excluded at 95% confidence level for gluino masses below 2100 GeV, and gluino $c\tau$ between 0.3 and 30 m. Another study, making use of a deep neural network to identify LLP decays, tagged by trackless and out-of-time jets [77], produced exclusion bounds at 95% confidence level, for neutralino production with masses below 1.18 TeV and $c\tau \approx 0.5$ m. More recently similar studies have been conducted also for HCAL, with the purpose of introducing for Run 3 a Level-1 trigger, processing data at 40MHz, to identify delayed jets, as signature of LLP [78], leveraging on the Phase 1 upgrade of HCAL, thanks to a new version of the HCAL QIE readout, integrating a TDC that can be used in the hardware trigger. The status-of-the-art has been summarized [79] at CALOR-24 (Tsukuba), and ICHEP-24 at Prague [80]. The trigger applies to the hadronic barrel (HB) calorimeter; there are reasons for considering the HF calorimeters as potential candidates for "delayed" jet investigations as well.

4.4 HF potential for "delayed jets" signatures

Up to now little attention was addressed to the HF calorimeters for "delayed" jet investigations. These modules have potentially excellent intrinsic time properties due to:

- Cherenkov light radiation and collection
  - Quartz fibers (prompt light emission; fast and stable light transmission)
  - fast PMT (sub-ns time resolution)
- Long baseline (11 m from IP5)

The time distribution of HF signals is highly concentrated (Figure 7, right) compared to the HB distribution and is well contained in a 25 ns interval, which corresponds to the separation of 2 bunch crossing in LHC.

Direct inspection of the shapes of individual pulses is even more instructive (Figure 8): with the new R7600U-100-M4 PMT, the pulse shape of the shower signals in HF (left) is much faster, with rise-time $t_R \approx 1.5$ ns. The right plot represents the signals that are occasionally produced by muons reaching directly the HF PMTs, and producing Cherenkov light in their photocathode glass window. These signals are extremely sharp, with $t_R \leq 1$ ns, and are recognized thanks to the redundant readout of the HF fibers (long/short fibers for EM and hadronic showers respectively) [82].

The time spread $\sigma_t = (\sigma_N / A_{max})\ t_R$, depends on the rise time t_R and signal-noise ratio (SNR) of the pulses, giving respectively $\sigma_t \approx 150$ ps for HF regular showers and $\sigma_t \approx 50$ ps for "window" signals in HF. In standard acquisition mode during data taking in LHC runs, the QIE-10 system used for HF provides data readout at 40 MHz with improved dynamic range

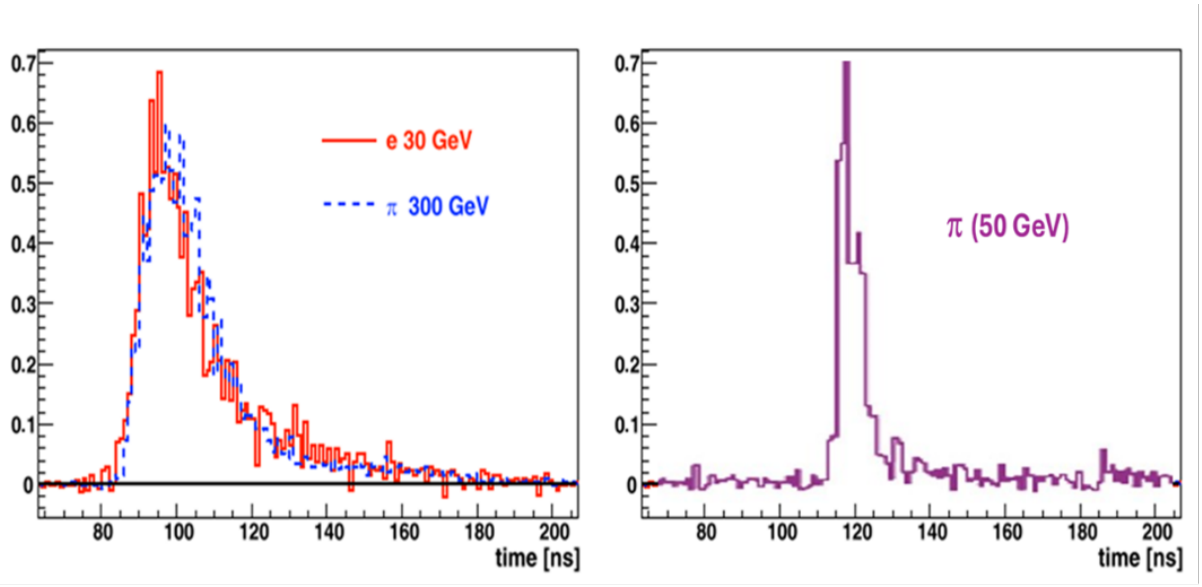

Figure 7: Time sampling of HB signal amplitudes (left) compared with the corresponding HF signals (right) for electron/pion showers and pion showers respectively, measured with R7525 PMT for HF and DEP HPD for HB [81].

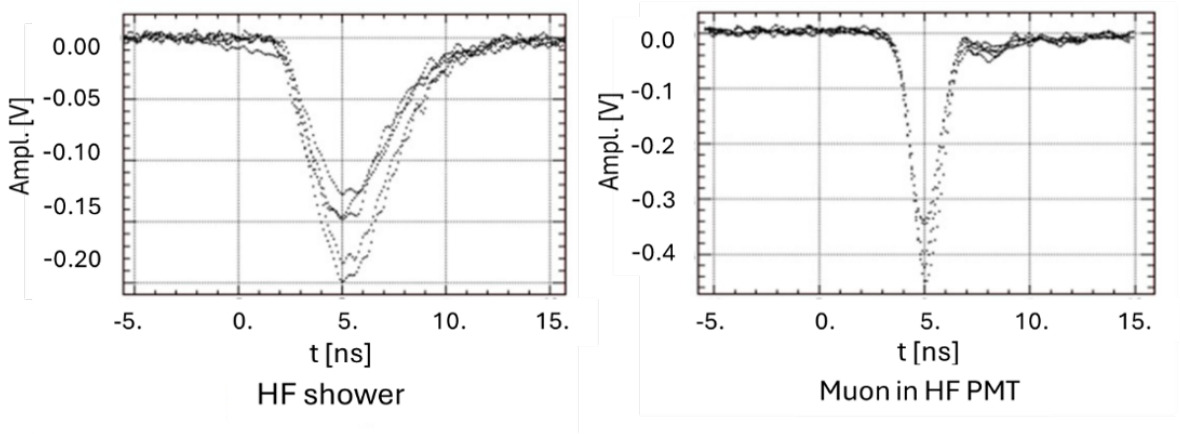

Figure 8: The pulse shape of HF shower signals (left) and "window" signals (right) for muons hitting the HF PMT, measured with R7600U-100-M4 PMT for HF and HPD for HB [83].

and a built-in TDC with 0.5 ns binning of a 25 ns interval. The nominal sensitivity of QIE10 is 3.1 fC/count and the nominal maximum charge that can be digitized is approximately 350 pC, yielding a nearly 17-bit dynamic range [84]. The ADC–TDC distribution of a single HF channel is in Figure 9 and shows very clear bands for the "window" event at and early time, and a swarm of "prompt" particles ($\beta \approx 1$). Late particles ($\beta << 1$) show up in the upper region, behind about 10 ns [85].

5 LLP Signals in HF

A signature for LLP BSM candidates $\mathcal{X}$, decaying to SM particles a and b ($\mathcal{X} \to a + b$) may come from their decay products, delayed with respect to the swarm of prompt particles ($\beta \approx 1$) from the IP, either by a potentially slower motion of the LLP up to the decay position, and an additional time for the decay products to reach the detectors, or both [74]. In Figure 10 such a

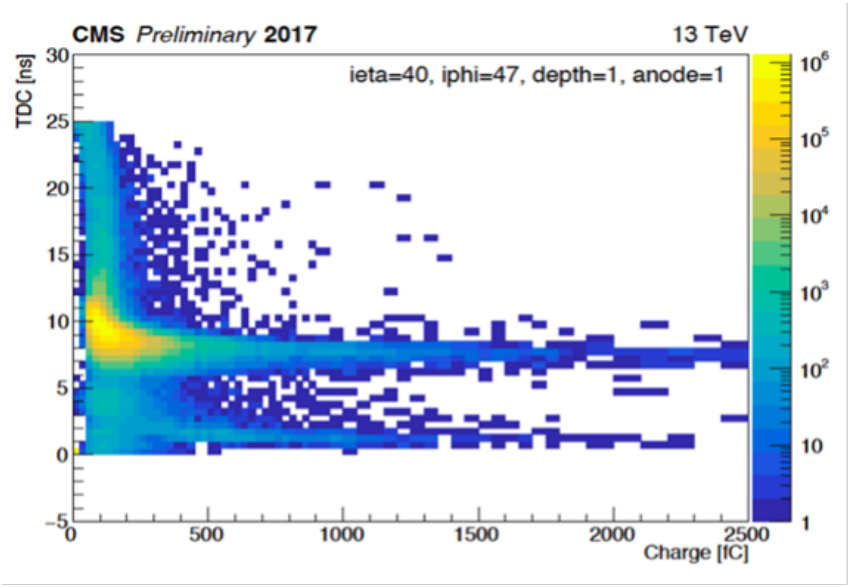

Figure 9: Time as measured by TDC vs anode charge in a given HF channel (ieta=40, iphi=47, depth=1). The contribution with low time values of < 5 ns originate from particles directly hitting the PMT. Hits from collision particles populate timing values of around 8 ns [85].

situation is represented for the region of the HF calorimeters ($3 \leq |\eta| \leq 5.2$) at about 11 m from IP5. Depending on specific properties of particle $\mathcal{X}$, it has been argued, f.i. in a recent physics survey for a Forward Physics Facility at the HL-LHC [17], that this kind of particles might be preferentially produced at larger $|\eta|$, escaping observation in the central detectors of the LHC experiments.

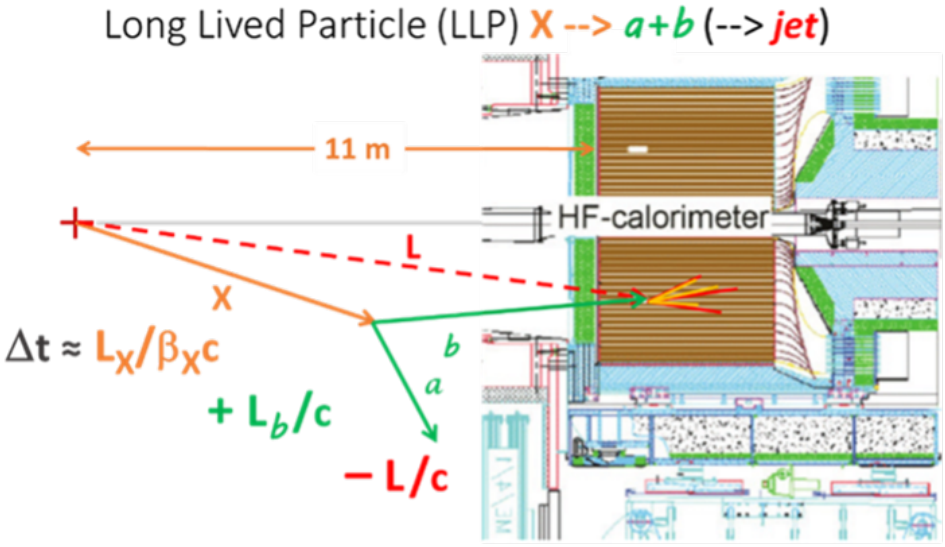

Figure 10: A sketch of a LLP particle $\mathcal{X}$ ($\rightarrow a + b$) , producing a "delayed" jet shower in HF.

5.1 Additional Tools

While the intrinsic timing properties of HF are well adapted for searches of events displaying "non-standard" time properties, resulting from "slow", weakly interacting, particles that can travel substantial distances, before decaying to particles, one of which, at least, would reach the HF module, with a substantial delay. The sensitivity to such events is determined by a time

resolution as small as possible, in order to catch even early late runners. As general comment, the presence of the "window" events, considered as a disturbing noise effect, would be useful to provide a valuable time reference for the "delayed" shower signals, mitigating potential sources of background described below.

5.2 Possible backgrounds

Possible fake "delayed" jet signature may be produced by 2 different features of the HF fibers and photodetectors:

- Afterpulses in the HF PMT
- Different fiber lengths in HF structure

Both these potential show-stoppers of employing HF for LLP hunting, are less serious than they appear initially:

- Rates of afterpulses have been measured for the HF PMTs, starting with the R7525 old type of PMT, showing characteristic bands of afterpulses as in Figure 11 (left), that have been associated with H2+ ($\approx$ 200ns), He+ ($\approx$ 400ns), and CH4+ ($\approx$ 700ns) [86, 87].
- On the other hand the R7600 PMT (metal channel dynode structure) did not show any afterpulse activity, even after a period of exposure to He gas (flowing for 3 weeks, and successive 3 weeks absorption), regularly monitored.
- Additionally the afterpulse spectrum is not expected to reach large amplitudes and therefore a mild amplitude cut would suppress this background almost completely.

The issue with the fiber lengths in the various HF towers is that all the fiber bundles equipping the towers of each HF wedge, have lengths slightly different; differences in different towers are not a problem, because each tower signal would simply have a different average delay, but length differences of fibers in one tower, contribute to the time spread of the tower signal.

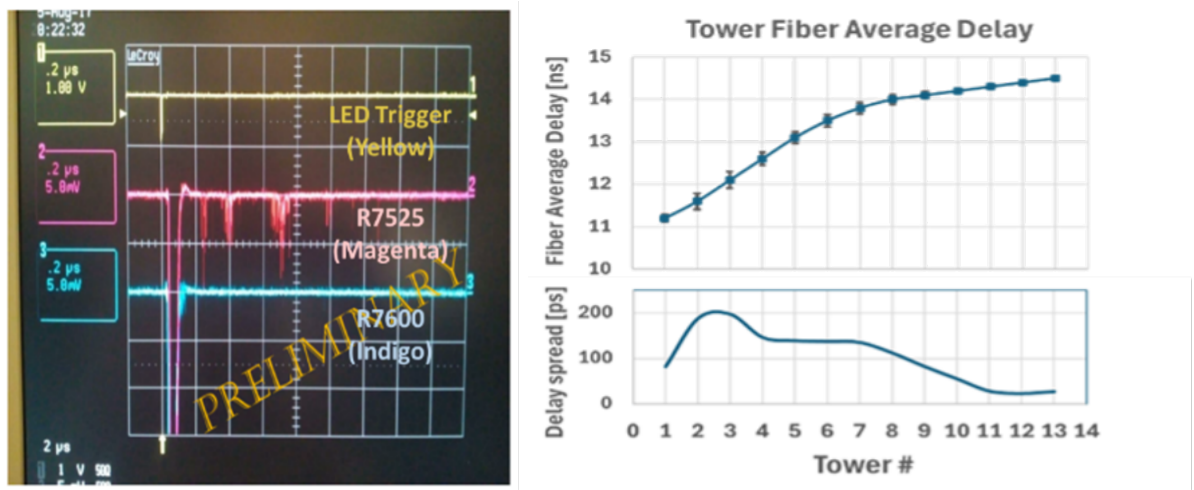

Figure 11: (Left) Afterpulses in R7525 PMT, magenta, showing clear bands of delayed pulses at $\approx$ 200ns, $\approx$ 400ns and $\approx$ 700ns associated respectively with H2+, He+ and CH4+ [86, 87]. The R7600 PMT (of the type now installed on HF) doesn't display any afterpulse activity [88]. (Right) The average delay of the fibers in specific HF towers; the vertical bars represent the spread of the fibers in the tower. The lower plot represents the spread of the length and delay of each tower.

5.3 Interim conclusions on LLP for HF

For the large towers, with many fibers, this spread has been estimated statistically; for the small towers, the few fibers have been arithmetically averaged; the average fiber lengths for each tower, are summarized in Figure 11 (right) and the spread within a tower is represented below.

It turns out that the (geometrical) spread in fibers' delays remains below 200ps, while measurements of the response of HF fibers to MIP particles, indicate time resolutions of the same order. As a conclusion: the spread in fiber length within a single tower in HF, doesn't spoil the intrinsic resolution of timing, possibly increasing it by a factor $\sqrt{2}$.

In conclusion HF, as is, seem adequate for a search of "delayed" jets, as signature for LLP production and decay. The TDC 500 ps binning might be coarser than the resolution achievable with HF, but sufficient for an initial approach.

6 Forward Aperture CMS Extension (FACET)

Continuing the exploration of the CMS forward region, a novel project can be considered, which is proposed as a CMS extension, to be located in one of the "dogleg" drift regions between D1 and the TAN (TAXN at HL-LHC) absorber where the ZDC is housed (Figure 12).

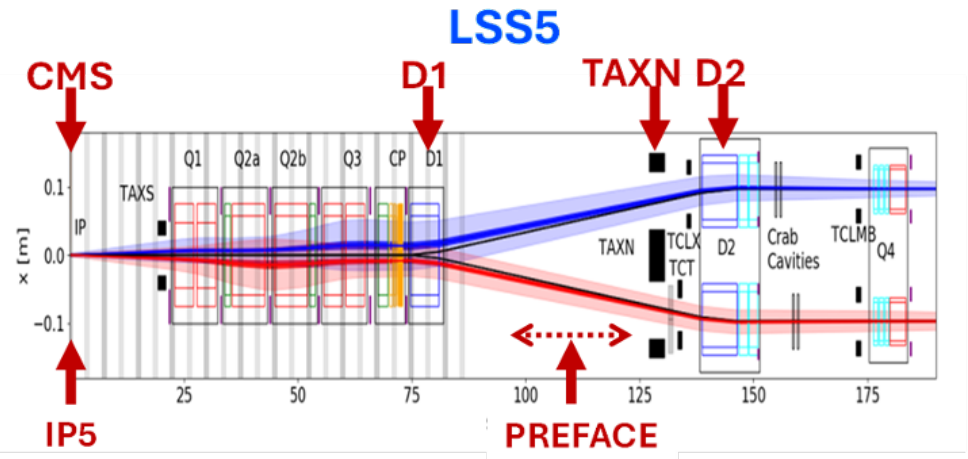

Figure 12: The scheme of the Long Straight Section at Point 5; CMS is to the left side; the region indicated, between D1 and TAXN represent an interesting area where it was proposed to install a setup with tracking, calorimetry and spectrometer to study very forward particle production and LLP searches [88].

6.1 The FACET apparatus

The proposed apparatus, FACET [89] is shown in Figure 13, and features:

- an enlarged beam pipe with radius r = 0.5 m, between z = 101-119 m, as decay volume;
- following the decay volume, a detector package consisting of
  - silicon trackers ($\sigma_{x,y} = 30\ \mu m$),
  - a timing layer ($\sigma_t \sim 30$ ps) and
  - a high granularity EM and hadronic calorimeter,

- followed by a permanent magnet spectrometer.

The background is greatly reduced because of 200-300 λ_{int} of magnetized iron in the LHC quadrupole magnets Q1-Q3, and LHC quality vacuum (10^{-7} - 10^{-9} Pa) in the decay volume.

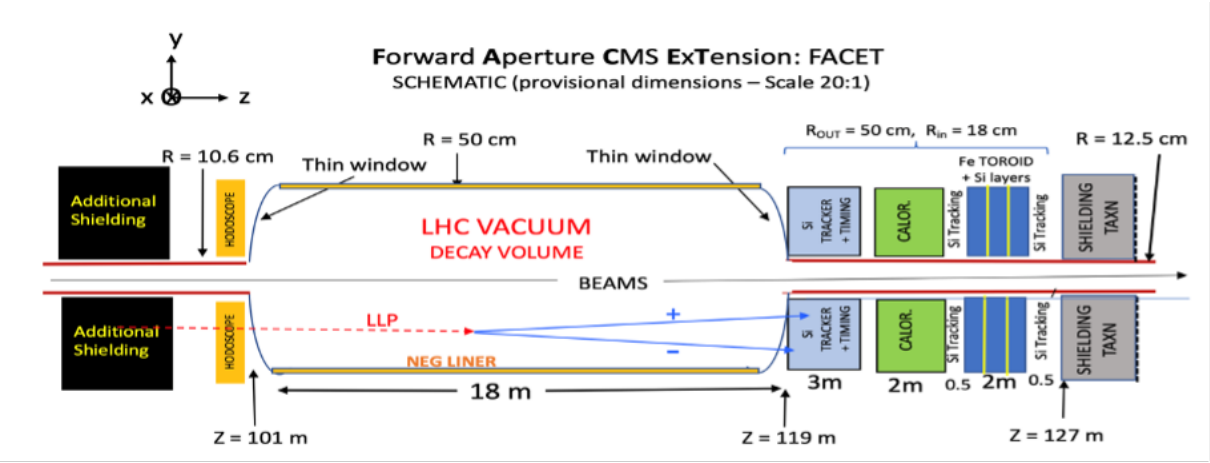

Figure 13: Schematic layout of the proposed FACET spectrometer.

6.2 The status of FACET

The physics case for FACET has been described in [89], and the project has attracted interest in the context of general and specific studies of LLP production via different portals [90, 91]. The comparison with FASER/FASER2 and other different proposed LLP detectors has been favourable to FACET in benchmark studies. Initially the project was aimed at the initial HL-LHC Run 4, but the special enlarged beam pipe is not foreseen for Run 4, therefore FACET as such, may be proposed only for Run 5. Different criteria can be considered for an optimization of the experimental setup compatible with the standard beam pipes, using a relatively large region above the pipe, that might be available for installation of detectors in LSS5 during LS3. Such a simplified version of FACET, compatible with the beam pipe design for Run 4, and with limited azimuthal coverage, may be considered as a technical demonstrator apparatus (PREFACE), preliminary to the full sized FACET detector for Run 5, aiming at prospecting the chosen LSS5 location in view of determining the appropriate running conditions and the performance of the technology solutions envisaged; even with modest instrumentation, some physics goals are considered, to have an initial flavour of the LLP phenomenology.

7 Conclusions

The cosmos has been sending to the Earth encrypted messages that are still waiting for clear interpretations; on a human scale enormous progress has been done in measuring all the components (electromagnetic, leptonic and hadronic) of the cosmic radiation, with surface detectors and with space instruments, and in approaching with man-made accelerators the energy scales typical of galactic and extragalactic sources. The energy gap is still huge, but the progress is impressive, and with the LHC it is possible to investigate the regime of the "knee" in the Cosmic Ray spectrum. Eventually the border region between cosmic ray and accelerator energies, may become a rich territory for QCD tests in novel conditions. Another type of galactic message is the overwhelming presence of dark matter (and energy) in the universe, making our (Standard Model) world look rather small.

Twelve years after the Higgs discovery, and extensive campaigns to search for phenomena beyond the Standard Model, no sign of BSM particles and/or new physics has appeared and the LHC experiments continue producing more and more precise proofs of validity for the Standard Model. It has been argued that new particles might escape observation, either populating phase-space corners less equipped in the standard LHC experiments (for instance the far-forward collision direction, along the beam pipes, or/and behaving in a drastically different manner than SM particles. The high-η region of CMS is only partially equipped, but it may be interesting to rely on the existing detectors, eventually completing them as much as possible, to search unconventional signatures. Two examples of instruments that might be able to detect and measure such unconventional signatures have been described briefly and their possibilities are under investigation.

Acknowledgments

The author would like to congratulate in the first place Prof. S. Narison, the Committees and the staff of QCD-24 for the organization and scientific level of this Conference. Special thanks to M. G. Albrow for inspiring discussions, to Y. Onel for valuable advice and support and to S.Hatipoglu, B. Kaynak, A. Mestvirishvili, M. Ovchynnikov, S. Ozkorucuklu and O. Potok for help and comments. Some topics connected to subjects of this paper have been developed by individuals or groups within the CMS HCAL and the CMS PPS/TOTEM communities: relevant members thereof (M. Arneodo, A. Belloni, K. Cankocak, S. Cerci, M. Deile, E. Gulmez, A. Kaminskiy, G.B. Kopp, M. Pitt, V. Samoylenko, A. Skuja, A. Stepennov, A. Toropin, C. Tully) are herewith duly acknowledged. The FACET project has been initiated by M.G. Albrow and developed thanks to notable contributions by F. Cerutti, D.R. Green, B. Hacisahinoglu, G. Landsberg, D. Lazic, M. Sabaté-Gilarte and D. Sunar Cerci, among others. This work was supported in part by the US Department of Energy under grant DE-SC0010113.

References

[1] A. Penzo, V. Samoylenko, and S. Sen, "Diffractive and parton processes with forward detectors at the LHC", *Nucl. Part. Phys. Proc.* **282–284** (2017) 15–19.

[2] CMS Collaboration, "The CMS experiment at the CERN LHC", *J. Instrum.* **3** (2008) 08004.

[3] L. Evans and P. Bryant, "Lhc machine", *JINST* **3** (2008) S08001.

[4] R.-D. Heuer, "Physics results at the LHC and implications for future high-energy physics programmes", in *Proc. of IPAC2012, New Orleans, Louisiana, USA*. IPAC'12 OC / IEEE, 2012.

[5] A. G. Myagkov, "Recent results from LHC experiments", *Phys. of Part. and Nucl. Lett.* **20** (2023), no. 3, 195–201.

[6] A. D. Roeck, M. P. Altarelli, and P. Savard, "Physics Results; Chapter 4 of "The Future of the Large Hadron Collider: A Super-Accelerator with Multiple Possible Lives"". World Scientific, Singapore, 2023. doi:10.1142/13513, ISBN 9789811280177.

[7] ATLAS Collaboration, "Observation of a new particle in the search for the standard model higgs boson with the ATLAS detector at the LHC", *Phys. Lett. B* **716** (2012) 1–29.

[8] CMS Collaboration, "Observation of a new boson at a mass of 125 gev with the CMS experiment at the LHC", *Phys. Lett. B* **716** (2012) 30–61.

[9] M. K. Gaillard, P. D. Grannis, and F. J. Sciulli, "The standard model of particle physics", *Rev. Mod. Phys.* **71** (1999) S96.

[10] "The standard model of particle physics", *Nature* **448** (2007) 270.

[11] T. W. B. Kibble, "The standard model of particle physics", *European Review* **23** (2014), no. 01, doi:10.1017/S1062798714000520, arXiv:1412.4094.

[12] G. Degrassi et al., "Higgs mass and vacuum stability in the standard model at nnlo", *J High Energy Phys.* **08** (2012) 098.

[13] A. Wulzer, "BSM lessons from the SM Higgs", in *Proc. of Eur. Phys. Soc. Conf. on High Energy Physics (EPS-HEP2015)*, volume PoS (EPS-HEP2015), p. 005. Vienna, Austria, October, 2015. arXiv:1510.05159v1.

[14] G. Bhattacharyya, "Hierarchy problem and BSM physics", *Pramana – J. Phys.* **89** (2017) 53, doi:10.1007/s12043-017-1448-2.

[15] E. Gibney, "The standard model is not dead': ultra-precise particle measurement thrills physicists", *Nature* **633** (2024) 745.

[16] L. Soffi (on behalf of ATLAS and CMS Collaborations), "Experimental overview of BSM searches (includes resonant HH production)", in *Presented at ICHEP2024 - 42nd Int. Conf. High Energy Phys.* Prague, Czech Republic, July, 2024. CMS CR -2024/169 (Aug 2024); To appear in Proc. of Phys.

[17] J. L. Feng et al., "The forward physics facility at the high-luminosity LHC", *J. Phys. G: Nucl. Part. Phys.* **50** (2023) 030501, doi:10.1088/1361-6471/ac865e.

[18] J. G. de Swart, G. Bertone, and J. van Dongen, "How dark matter came to matter", *Nature Astronomy* **1** (2017) 0059.

[19] G. Arcadi, "Dark Matter through the Higgs portal", *Physics Reports* **842** (2020) 1–180.

[20] Juliette Alimena et al., "Searching for long-lived particles beyond the standard model at the large hadron collider", *J. Phys. G: Nucl. Part. Phys.* **47** (2020) 090501.

[21] G. Galilei, "Sidereus Nuncius". Thomas Baglioni, Venice, Italy, 1610.

[22] I. Hook and the OPTICON ELT Science Working Group, "Science with extremely large telescopes", *The Messenger* **121** (September, 2005) 2–10.

[23] N. English, "Space Telescopes – Capturing the Rays of the Electromagnetic Spectrum". Springer, Cham, 2017. ISBN 978-3-319-27812-4.

[24] F. Giovannelli and L. Sabau-Graziati, "Multifrequency astrophysics today", *Chinese Journal of Astronomy and Astrophysics* **3** (2003), no. S1, 1–29.

[25] V. F. Hess, "Über beobachtungen der durchdringenden strahlung bei sieben freiballonfahrten", *Physikalische Zeitschrift* **13** (1912) 1084–1091.

[26] C. D. Anderson, "The positive electron", *Physical Review* **43** (1933), no. 6, 491–494.

[27] C. D. Anderson and S. H. Neddermeyer, "Cloud chamber observations of cosmic rays at 4300 meters elevation and near sea level", *Physical Review* **50** (1936), no. 4, 263–271.

[28] C. M. G. Lattes, G. P. S. Occhialini, and C. F. Powell, "Observations on the tracks of slow mesons in photographic emulsions", *Nature* **160** (1947), no. 4067, 486–492.

[29] O. Chamberlain, E. Segrè, C. Wiegand, and T. Ypsilantis, "Observation of antiprotons", *Physical Review* **100** (1955), no. 3, 947.

[30] P. Auger, R. Maze, and A. F. Robley, "Extension et pouvoir pénétrant des grandes gerbes de rayons cosmiques", *Comptes Rendus* **208** (1939) 1641.

[31] A. Watson, "A brief history of the study of high energy cosmic rays using arrays of surface detectors", in *UHECR 2022; EPJ Web of Conferences*, volume 283, p. 01002. 2023.

[32] D. d'Enterria et al., "Constraints from the first LHC data on hadronic event generators for ultra-high energy cosmic-ray physics", *Astroparticle Physics* **35** (2011), no. 2, 98–113, arXiv:1101.5596.

[33] K. Greisen, "End to the cosmic-ray spectrum?", *Physical Review Letters* **16** (1966) 748–750.

[34] G. T. Zatsepin and V. A. Kuzmin, "Upper limit of the spectrum of cosmic rays", *Journal of Experimental and Theoretical Physics Letters* **4** (1966) 78.

[35] M. Boezio, R. Munini, and P. G. Picozza, "Cosmic ray detection in space", *Progress in Particle and Nuclear Physics* **112** (2020) 103765.

[36] A. V. Olinto et al. (POEMMA Collaboration), "The POEMMA (Probe of Extreme Multi-Messenger Astrophysics) Observatory", *Journal of Cosmology and Astroparticle Physics* **06** (2021) 007, doi:10.1088/1475-7516/2021/06/007.

[37] E. Fermi, "On the origin of cosmic radiation", *Physical Review* **75** (1949) 1169–1174.

[38] A. Coleman et al., "Ultra-high-energy cosmic rays: The intersection of the cosmic and energy frontiers (white paper snowmass 2021)", *Astroparticle Physics* **149** (2023) 102819, doi:10.1016/j.astropartphys.2023.102819, arXiv:2205.05845.

[39] P. Mészáros, D. B. Fox, C. Hanna, and K. Murase, "Multi-messenger astrophysics", *Nature Reviews Physics* **1** (2019), no. 10, 585–599, doi:10.1038/s42254-019-0101-z.

[40] J. R. Hörandel, "On total inelastic cross sections and the average depth of the maximum of extensive air showers", *J. Phys. G: Nucl. Part. Phys.* **29** (2003) 2439, doi:10.1088/0954-3899/29/11/001.

[41] R. J. Glauber and G. Matthiae, "High-energy scattering of protons by nuclei", *Nuclear Physics B* **21** (1970), no. 2, 135–157, doi:10.1016/0550-3213(70)90511-0.

[42] The CMS Collaboration, "Measurement of isolated photon production in pp and PbPb collisions at $\sqrt{s_{\mathrm{NN}}}$ = 2.76 TeV", *Phys. Lett. B* **710** (2012) 256, arXiv:1201.3093v2. CERN-PH-EP/2011-22; CMS-HIN-11-002.

[43] The TOTEM Collaboration, "The TOTEM Experiment at the CERN Large Hadron Collider", *JINST* **3** (2008) S08007.

[44] CMS Collaboration, "The CMS Precision Proton Spectrometer at the HL-LHC Expression of Interest", 2021.

[45] F. S. Cafagna (for the TOTEM Collaboration), "Latest results for proton-proton Cross Section Measurements with the TOTEM experiment at LHC", in *36th Int. Cosmic Ray Conf. -ICRC2019, Madison, WI, U.S.A*, volume PoS(ICRC2019), p. 207. 2019.

[46] D0 and TOTEM Collaborations, "Comparison of pp and $p\bar{p}$ differential elastic cross sections and observation of the exchange of a colorless C-odd gluonic compound", *Phys. Rev. Lett.* **127** (2021) 062003, arXiv:2012.03981.

[47] The CMS Collaboration, "Measurement of the inelastic cross section in proton-lead collisions at $\sqrt{s_{\mathrm{NN}}}$ = 5.02 TeV", *Phys. Lett. B* **759** (2016) 641–662, arXiv:1509.03893v2.

[48] M. Grothe, "Forward detectors around the CMS interaction point at LHC and their physics potential", in *Proc. High-energy photon collisions at the LHC, CERN, CH*, volume CMS CR-2008/033, pp. Nucl.Phys.Proc.Suppl.179–180:173–180. 2008. arXiv:0806.2977. doi:10.1016/j.nuclphysbps.2008.07.022.

[49] M. Albrow, "A Very Forward Hadron Spectrometer for the LHC and Cosmic Ray Physics", in *2nd World Summit: Exploring the Dark Side of the Universe*. University of Antilles, Pointe-a-Pitre, Guadeloupe, France, 2018. arXiv:1811.02047v1. 5 Nov 2018.

[50] J. Pinfold, "ATLAS and ultra high energy cosmic ray physics", *EPJ Web of Conferences* **145** (2017) 10001, doi:10.1051/epjconf/201714510001.

[51] C. Baus, "Measurements in the Forward Phase-Space with the CMS Experiment and their Impact on Physics of Extensive Air Showers". PhD thesis, CERN, 2015. CERN-THESIS-2015-222.

[52] David d'Enterria et al., "The Strong Interaction at the Collider and Cosmic-Rays Frontiers", *Few-Body Systems* **53** (2012) 173–179, doi:10.1007/s00601-011-0255-4.

[53] A. Aab et al. (The Pierre Auger Collaboration), "Testing Hadronic Interactions at Ultrahigh Energies with Air Showers Measured by the Pierre Auger Observatory", *Phys. Rev. Lett.* **117** (2016) 192001, arXiv:1610.08509v2.

[54] D. d'Enterria, "Ultrahigh-energy cosmic rays: Anomalies, QCD, and LHC data", in *Ultra High Energy Cosmic Rays 2018 (UHECR 2018)*, volume 210, p. 02005. 2019. arXiv:1902.09505v2. doi:10.1051/epjconf/201921002005.

[55] Alves Batista R et al., "Open Questions in Cosmic-Ray Research at Ultrahigh Energies", *Front. Astron. Space Sci.* **6** (2019) 23, doi:10.3389/fspas.2019.00023.

[56] A. Aab et al. (Pierre Auger Collaboration), "Muons in air showers at the Pierre Auger Observatory: Mean number in highly inclined events", *Phys. Rev. D* **91** (2015) 032003. Erratum Phys. Rev. D 91, 059901 (2015).

[57] A. A. Petrukhin, "Muon Puzzle in Cosmic Rays and Its Possible Solution", *Phys. Atom. Nuclei* **84** (2021) 92–99, doi:10.1134/S1063778821010142.

[58] J. Albrecht et al., "The Muon Puzzle in cosmic-ray induced air showers and its connection to the Large Hadron Collider", *Astrophys Space Sci* **367** (2022) 27, doi:10.1007/s10509-022-04054-5.

[59] R. Scaria et al., "Muon Puzzle: Bridging the gap between cosmic ray and accelerator experiments", in *Proc. 38th Int. Cosmic Ray Conf. (ICRC2023)*, volume PoS(ICRC2023), p. 518. 2023.

[60] S. Abatzis et al. [WA85 Collaboration], "Ξ^-, anti-Ξ^-, Λ and anti-Λ production in Sulphur-Tungsten interactions at 200-GeV/c per nucleon", *Phys. Lett. B* **270** (1991) 123.

[61] ALICE Collaboration, "Enhanced production of multi-strange hadrons in high-multiplicity proton–proton collisions", *Nature Phys* **13** (2017) 535–539, doi:10.1038/nphys4111.

[62] A. M. Sirunyan et al. (CMS Collaboration), "Strange hadron production in pp and pPb collisions at $\sqrt{s_{\mathrm{NN}}} = 5.02$ TeV", *Phys. Rev. C* **101** (2020) 064906, doi:10.1103/PhysRevC.101.064906.

[63] F. Zwicky, "On the masses of nebulae and of clusters of nebulae", *Astrophysical Journal* **86** (1937) 217, doi:10.1086/143864.

[64] V. Rubin and J. W. Kent Ford, "Rotation of the andromeda nebula from a spectroscopic survey of emission regions", *The Astrophysical Journal* **159** (1970) 379.

[65] A. Canepa, "Searches for supersymmetry at the large hadron collider", *Reviews in Physics* **4** (2019) 100033.

[66] Y. A. Abulaiti (on behalf of ATLAS and CMS collaborations), "Status of searches for dark matter at the LHC", in *Rencontres de Blois 2021*, volume ATL-PHYS-PROC-2022-003. 2022.

[67] A. Hayrapetyan et al. (CMS Collaboration), "Dark sector searches with the CMS experiment", *Submitted to Physics Reports* (2024) arXiv:2405.13778.

[68] M. Rauch, "Vector-Boson Fusion and Vector-Boson Scattering", arXiv:1610.08420. KA-TP-35-2016.

[69] S. Gori, Z. Liu, and B. Shakya, "Heavy Higgs as a portal to the supersymmetric electroweak sector", *JHEP* **04** (2019) 049.

[70] K. Cankocak et al., "Radiation-hardness Measurements of High-OH Content Fibers Irradiated with 24 GeV Protons up to 1.25 Grad", *Nucl. Instrum. Meth. A* **585** (2008) 20–27.

[71] B. Kaynak, S. Ozkorucuklu, and A. Penzo, "Measuring time with high precision in particle physics", *Radiat. Eff. Def. Solids* **177** (2022) 1320–1339, doi:10.1080/10420150.2022.2136093.

[72] A. Santocchia, "Searching for Long Lived Particles at LHC", 2024. CMS-CR-2024-219.

[73] Fabio Cossutti (CMS Collaboration), "Precision Timing with the CMS MIP Timing Detector for High-Luminosity LHC", in *42nd International Conference on High Energy Physics (ICHEP 2024)*. 2024.

[74] J. Liu, Z. Liu, and L.-T. Wang, "Enhancing Long-Lived Particles Searches at the LHC with Precision Timing Information", *Phys. Rev. Lett.* **122** (2019) 131801, arXiv:1805.05957.

[75] D. del Re, "Timing performance of the CMS ECAL and prospects for the future", *J. Phys. Conf. Ser.* **587** (2015) 012003, doi:10.1088/1742-6596/587/1/012003.

[76] CMS Collaboration, "Search for long-lived particles using nonprompt jets and missing transverse momentum with proton-proton collisions at $\sqrt{s} = 13$ TeV", *Phys. Lett. B* **797** (2019) 134876, doi:10.1016/j.physletb.2019.134876, arXiv:1906.06441.

[77] CMS Collaboration, "Search for long-lived particles using out-of-time trackless jets in proton-proton collisions at $\sqrt{s} = 13$ TeV", *JHEP* **07** (2023) 210, doi:10.1007/JHEP07(2023)210, arXiv:2212.06695.

[78] G. Kopp and C. Tully et al., "A Novel Timing Trigger with the CMS Hadron Calorimeter", 2023. CERN-CMS-DN-2023-022.

[79] G. Kopp et al., "Time Alignment of the CMS Hadron Calorimeter for a Novel Timing Trigger", in *CALOR 2024: 20th International Conference on Calorimetry in Particle Physics*. 2024. Tsukuba, Japan.

[80] G. Kopp, "Long-Lived Particle Triggering with the CMS Hadron Calorimeter", in *ICHEP 2024*. 2024.

[81] CMS Collaboration, "Performance of CMS Hadron Calorimeter Timing and Synchronization using Test Beam, Cosmic Ray, and LHC Beam Data", *JINST* **5** (2010) T03013, arXiv:0911.4877.

[82] A. Moeller et al., "Analysis of Abnormally High Energy Events in CMS Forward Calorimeters" (2008), Semantic Scholar (https://www.semanticscholar.org/paper/Analysis-of-Abnormally-High-Energy-Events-in-CMS-Moeller-Onel/fcf3886813471264f60304226eb5491c7a42b5ae)

[83] Ugur Akgun (for CMS Collaboration), "Detector Upgrade R&D of the CMS Hadronic Endcap and Forward Calorimeters", in *Nuclear Science Symposium Conference Record (NSS/MIC), 2009 IEEE*. 2009. doi:10.1109/NSSMIC.2009.5402384.

[84] A. Baumbaugh et al., "QIE10: A new front-end custom integrated circuit for high-rate experiments", *JINST* **9** (2013) C01062, doi:10.1088/1748-0221/9/01/C01062.

[85] A. Hayrapetyan et al. (CMS Collaboration), "Development of the CMS detector for the CERN LHC Run 3", *JINST* **19** (2024) P05064, doi:10.1088/1748-0221/19/05/P05064, arXiv:2309.05466v2.

[86] N. Akchurin and H.-J. Kim, "A study on ion initiated photomultiplier afterpulses", *Nucl. Instrum. Meth. A* **574** (2007) 121–126, doi:10.1016/j.nima.2007.01.093.

[87] U. Akgun et al., "Afterpulse timing and rate investigation of three different Hamamatsu Photomultiplier Tubes", *JINST* **3** (2008) T01001, doi:10.1088/1748-0221/3/01/T01001.

[88] R. Ospanov et al., "Studies of helium poisoning of a Hamamatsu R5900-00-M16 photomultiplier", 2019. arXiv:1908.08869v1.

[89] S. Cerci et al., "FACET: a new long-lived particle detector in the very forward region of the CMS experiment", *J. High Energ. Phys.* **2022** (2022) 110.

[90] M. Ovchynnikov et al., "Sensitivity of the FACET experiment to Heavy Neutral Leptons and Dark Scalars", *Journal of High Energy Physics* **2023** (2023), no. 2,.

[91] M. Du et al., "Enhanced long-lived dark photon signals at lifetime frontier detectors", *Phys. Rev. D* **105** (2022) 055012.